Electronic Supplementary Material (ESI) for New Journal of Chemistry.

Supporting Information

Proton conduction studies on two nonporous coordination complexes with different proton density

Ying-Bing Lu*[, a], Xue-Lian Lin[a], Jia-Hao Ai[a], Yu-Zheng Cai [a], Shui-Qing Li[a], Rong Li*[, b], Shi-Yong Zhang[a], Yong-Rong Xie[a] and Shui-Dong Zhu*[,a]

[a]*Jiangxi Key Laboratory of Function of Materials Chemistry, College of Chemistry and Chemical Engineering, Gannan Normal University, Ganzhou, 341000, P. R. China.*

[b]*School of Metallurgy and Chemical Engineering, Jiangxi University of Science and Technology, Ganzhou 341000, Jiangxi Province, P. R. China.*

[c]*School of Materials Science & Engineering, Hubei University, Wuhan 430062, P. R. China*

E-mail: ybluhm@163.com, rli@hubu.edu.cn, zsd2002@sina.com.

Table S1. Various coordination modes of H_3CAM ligand (quoted from our previous literature[1])

Monodentate	Didentate	Tridentate			Tetradentate
1) 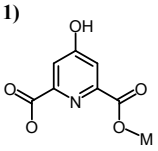	2) 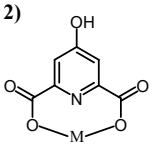	3) 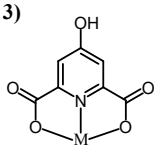	4) 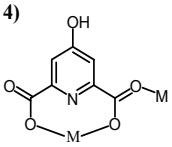	5) 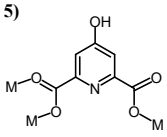	6) 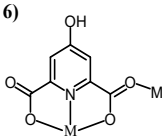 Complex **1** Complex **2**
			Pendentate		
7) 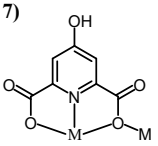	8) 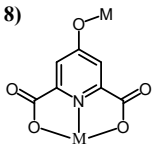 Complex **1**	9) 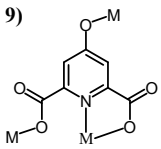	10) 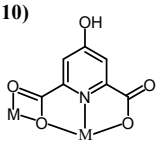	11) 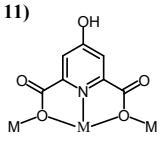	12) 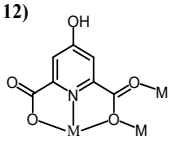
			Hexadentate		
13) 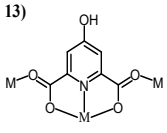	14) 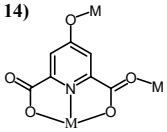	15) 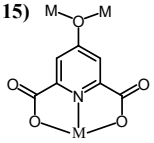	16) 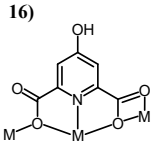	17) 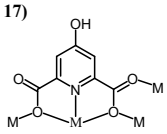	18) 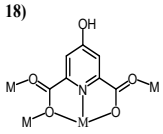

			Heptadentate		
19) 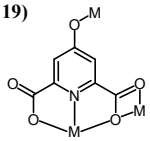	20) 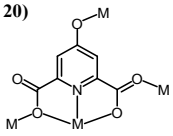	21) 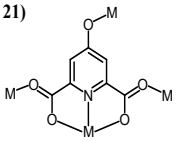	22) 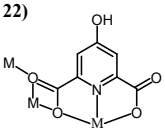	23) 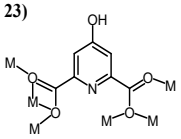	24) 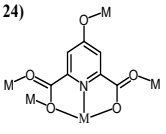
Octadentate		Nanodentate		Tendentate	Dodecadentate
25) 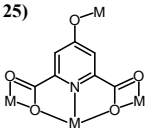	26) 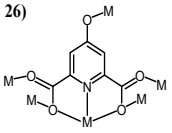	27) 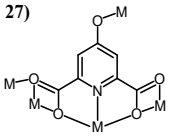	28) 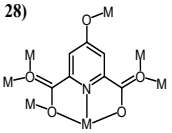	29) 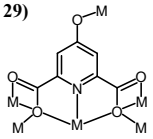	30) 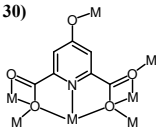

Table S2. Diverse deprotonated modes of H_3CAM ligand

L^{-1}		L^{-2}	L^{-3}		
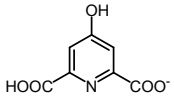	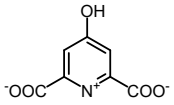	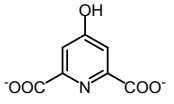	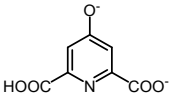	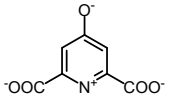	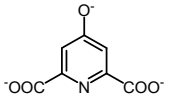

Table S3. Selected Bond Lengths (Å) and Bond Angles (°) for **1** and **2**

Complex **1**	Bond Lengths (Å)		
Cu(1)-O(10)#1	1.8768(19)	Cu(2)-N(2)	1.879(2)
Cu(1)-N(1)	1.894(2)	Cu(2)-O(4)	1.9008(19)
Cu(1)-O(3)	2.0642(19)	Cu(2)-O(8)	1.9919(19)
Cu(1)-O(1)	1.9797(19)	Cu(2)-O(6)	2.0678(19)
Cu(1)-Na(1)#2	3.2136(13)	Cu(2)-O(1W)	2.266(2)
Complex **1**	Bond Angles (°)		
O(10)#1-Cu(1)-N(1)	169.93(9)	N(2)-Cu(2)-O(4)	156.18(10)
O(10)#1-Cu(1)-O(3)	90.40(8)	N(2)-Cu(2)-O(8)	81.83(9)
N(1)-Cu(1)-O(3)	79.89(8)	O(4)-Cu(2)-O(8)	89.06(8)
O(10)#1-Cu(1)-O(1)	108.62(8)	N(2)-Cu(2)-O(6)	79.73(8)
N(1)-Cu(1)-O(1)	80.85(8)	O(2)-Cu(2)-O(6)	106.10(8)
O(3)-Cu(1)-O(1)	160.36(8)	O(8)-Cu(2)-O(6)	160.97(8)
O(10)#1-Cu(1)-Na(1)#2	52.53(6)	N(2)-Cu(2)-O(1W)	98.94(9)
N(1)-Cu(1)-Na(1)#2	120.08(7)	O(6)-Cu(2)-O(1W)	86.36(8)
Complex **2**	Bond Lengths (Å)		

Mn(1)-O(1)	2.0681(13)	Mn(2)-O(6)	2.0741(12)
Mn(1)-O(8)	2.1920(13)	Mn(2)-O(4)#1	2.1650(13)
Mn(1)-N(4)	2.2021(17)	Mn(2)-N(8)	2.1723(16)
Mn(1)-N(2)	2.2039(14)	Mn(2)-N(1)#1	2.2186(14)
Mn(1)-N(3)	2.2941(16)	Mn(2)-N(7)	2.4921(16)
Mn(1)-O(7)	2.4548(13)	Mn(2)-O(2)#1	2.5071(13)
Complex **2**	Bond Angles (°)		
O(1)-Mn(1)-O(8)	105.99(6)	O(6)-Mn(2)-O(4)#1	117.66(5)
O(1)-Mn(1)-N(4)	149.23(6)	O(6)-Mn(2)-N(8)	119.15(6)
O(8)-Mn(1)-N(4)	99.55(6)	O(4)#1-Mn(2)-N(8)	115.60(6)
O(1)-Mn(1)-N(2)	109.34(5)	O(6)-Mn(2)-N(1)#1	118.42(5)
O(8)-Mn(1)-N(2)	72.96(5)	O(4)#1-Mn(2)-N(1)#1	72.34(5)
N(4)-Mn(1)-N(2)	94.23(6)	N(8)-Mn(2)-N(1)#1	103.81(6)
O(1)-Mn(1)-N(3)	88.30(6)	O(6)-Mn(2)-N(7)	90.51(5)
O(8)-Mn(1)-N(3)	88.91(6)	O(4)#1-Mn(2)-N(7)	78.47(5)

Symmetry Codes for **1**, #1 $x-1/2, -y-7/2, z-1/2$; #2 $-x+3/2, y-1/2, -z+1/2$; #3 $-x+3/2, y+1/2, -z+1/2$; #4 $-x+2, -y-3, -z+1$; #5 $x-1/2, -y-7/2, z+1/2$;

For **2**, #1 : $x, y+1$, z; B: $x, y-1, z$;

Table S4. Summary of *SHAPE* analysis of Cu1 and Cu2 for **1**.

ion	label	shape	symmetry	Distortion(τ)
Cu1	PP-5	Pentagon	D5h	23.770
	vOC-5	Vacant octahedron	C4v	4.597
	TBPY-5	Trigonal bipyramid	D3h	8.613
	SPY-5	**Spherical square pyramid**	**C4v**	**3.960**
	JTBPY-5	Johnson trigonal bipyramid J12	D3h	11.730
	PP-5	Pentagon	D5h	27.800
	vOC-5	Vacant octahedron	C4v	2.727
Cu2	TBPY-5	Trigonal bipyramid	D3h	4.320
	SPY-5	**Spherical square pyramid**	**C4v**	**1.703**
	JTBPY-5	Johnson trigonal bipyramid J12	D3h	6.698

Table S5. H-bonding length and angle table for **1**.

D-H…A	d(H…A)(Å)	d(D…A)(Å)	<DHA(Å)
O1W--H1WA..O3	2.30	3.048(3)	142
O5--H3..O7	1.87(6)	2.694(3)	167(4)
O2W--H2WA.O7	2.06	2.792(4)	139
O2W--H2WB..O3	2.54	3.179(4)	129
O2W--H2WB..O4	2.14	2.971(4)	154
O1W--H1WB..O8	1.94	2.821(3)	175

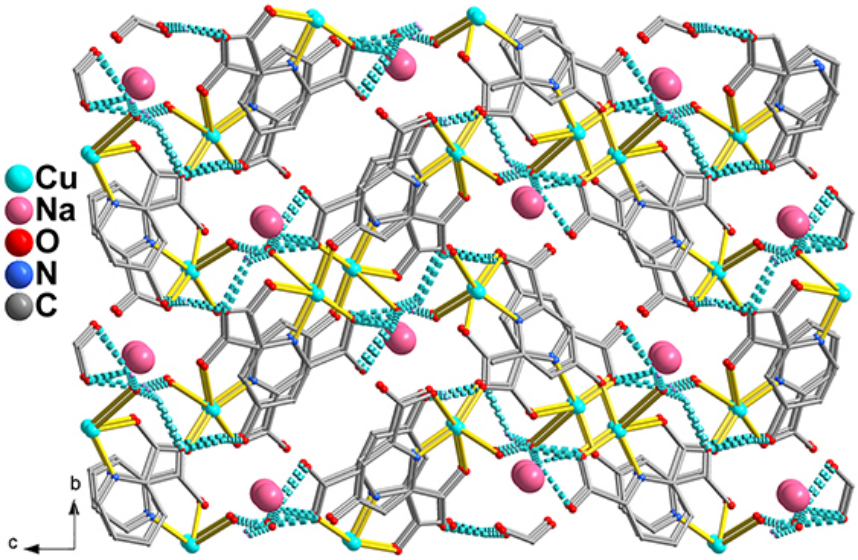

Figure S1. The 3D network of **1** in which the Na^+ cations filled in one channel along the *a* axis.

Table S6. Summary of *SHAPE* analysis of Mn1 and Mn2 for **2.**

ion	label	shape	symmetry	Distortion(τ)
	HP-6	Hexagon	D6h	33.642
	PPY-6	Pentagonal pyramid	C5v	14.648
Mn1	OC-6	Octahedron	Oh	7.812
	TPR-6	**Trigonal prism**	**D3h**	**6.216**
	JPPY-6	Johnson pentagonal pyramid J2	C5v	17.919
	HP-6	Hexagon	D6h	32.265
	PPY-6	Pentagonal pyramid	C5v	8.193
Mn2	OC-6	Octahedron	Oh	16.851
	TPR-6	**Trigonal prism**	**D3h**	**5.760**
	JPPY-6	Johnson pentagonal pyramid J2	C5v	11.578

Table S7. H-bonding length and angle table for **2**.

D-H…A	d(H…A) (Å)	d(D…A) (Å)	<DHA (Å)
O(5)-H(5)…O(7)	1.80	2.6176(18)	173
N(5)--H(5A)..O(8)	2.10	2.837(2)	143
N(5)--H(5A) ..O(9)	2.60	3.339(2)	145
N(6)--H(6)..O(9)	1.93	2.776(3)	170
N(9)--H(9A..O(3)	2.14	2.989(2)	167
N(9)--H(9A)..O(4)	2.58	3.129(2)	122
O(10)--H(10)..O(2)	1.82	2.6132(17)	161
N(10)--H(10A)..O(4)	2.17	2.892(2)	142

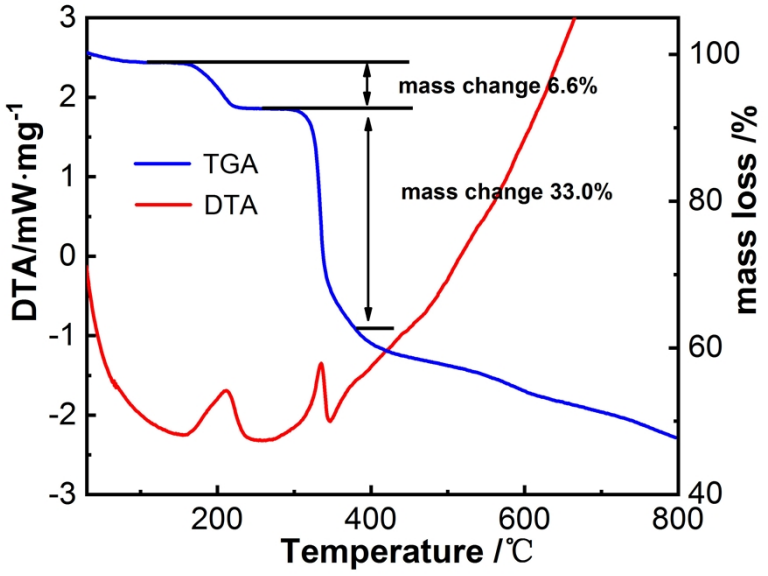

Figure S2. TGA and DTA of **1** from 30 °C to 800 °C

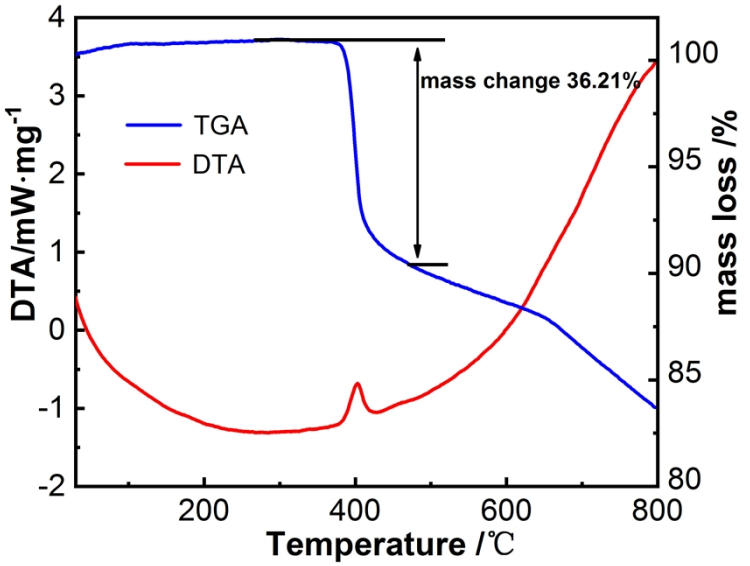

Figure S3. TGA and DTA of **2** from 30 °C to 800 °C

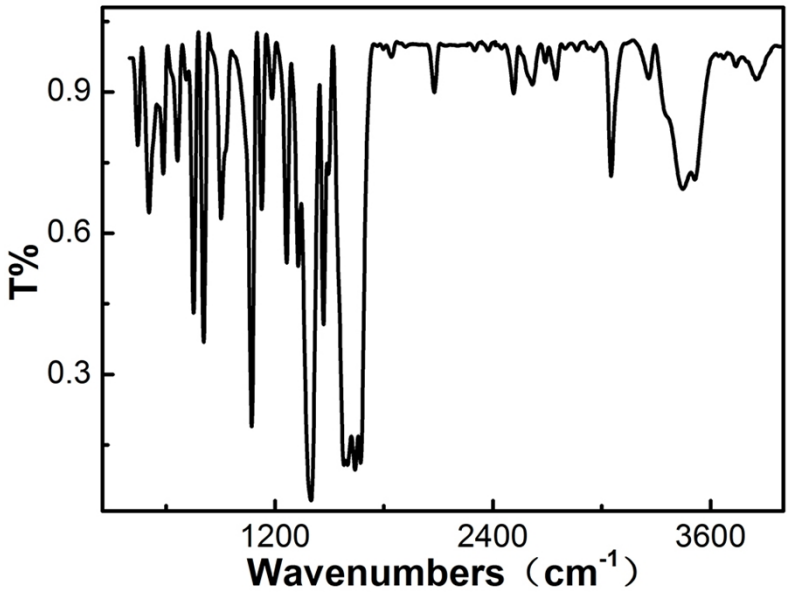

Figure S4. IR spectra for **1**.

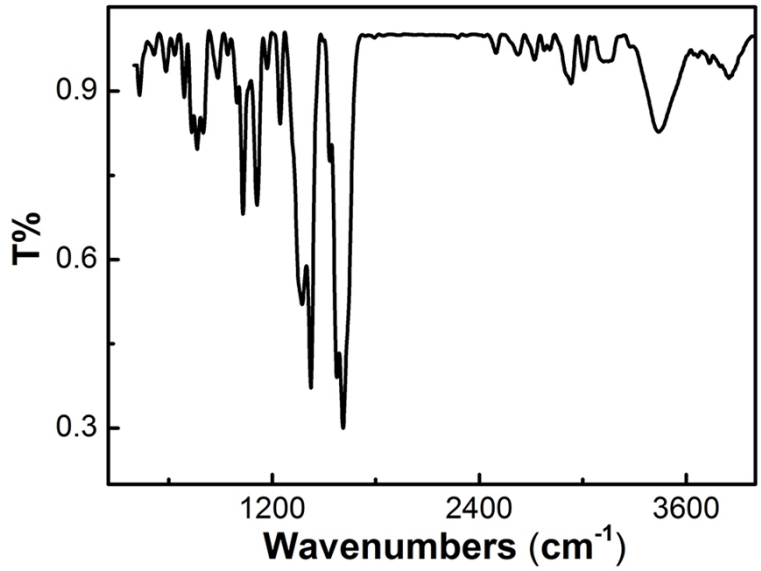

Figure S5. IR spectra for **2**.

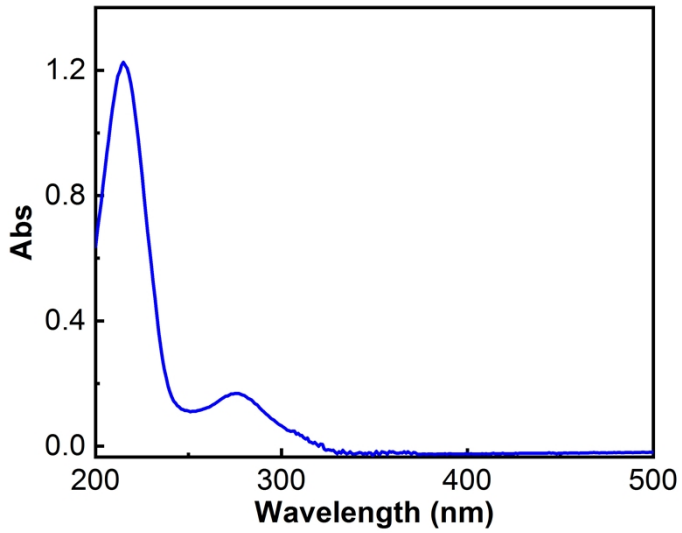

Figure S6. UV-vis spectra for **1**.

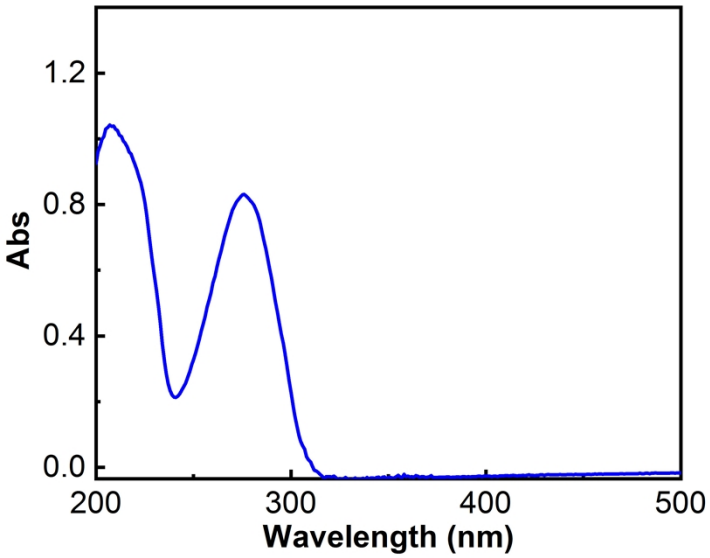

Figure S7. UV-vis spectra for **2**.

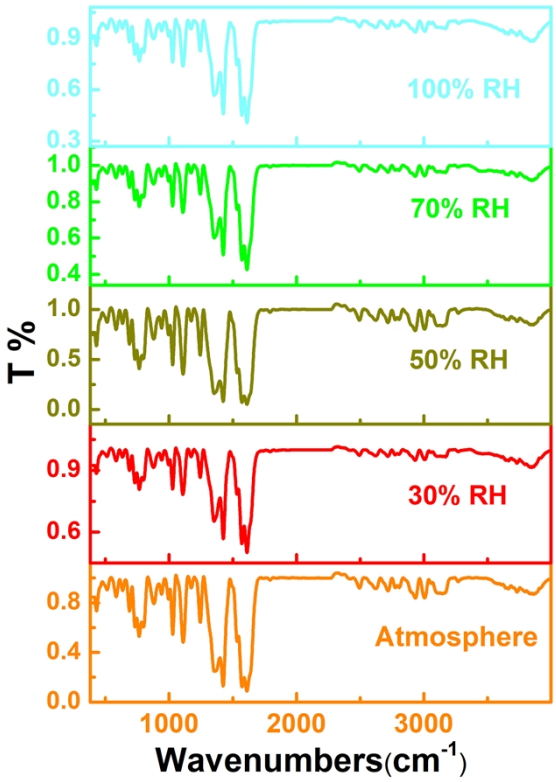

Figure S8. The IR spectra of **1** at 25 °C under different humidity (RH)

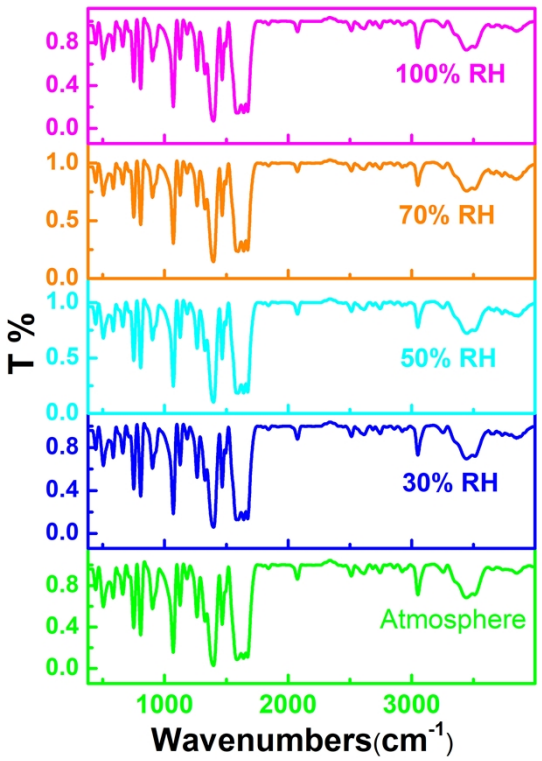

Figure S9. The IR spectra of **2** at 25 °C under different humidity (RH)

Table S8. The proton conductivity of **1** at 25 °C under variable relative humidity (RH).

RH / %	σ / S cm^{-1}
50	7.10×10^{-10}
60	3.04×10^{-9}
70	2.48×10^{-8}
80	1.18×10^{-7}
90	6.52×10^{-7}
100	5.22×10^{-6}

Table S9. The proton conductivity of **1** at 100 % under variable temperature (°C).

Temperature / °C	σ / S cm^{-1}
25	5.22×10^{-6}
40	1.51×10^{-5}
55	2.72×10^{-5}
70	4.72×10^{-5}
85	6.72×10^{-5}

Table S10. The proton conductivity of **2** at 25°C under variable relative humidity (RH).

RH / %	σ / S cm^{-1}
50	7.1×10^{-10}
60	1.59×10^{-9}
70	1.05×10^{-9}
80	2.16×10^{-7}
90	8.19×10^{-7}
100	3.27×10^{-5}

Table S11. The proton conductivity of **2** at 100 % under variable temperature (°C).

Temperature / °C	σ / S cm^{-1}
25	3.27×10^{-5}
40	4.18×10^{-5}
55	5.61×10^{-5}
70	7.05×10^{-5}
85	1.70×10^{-4}

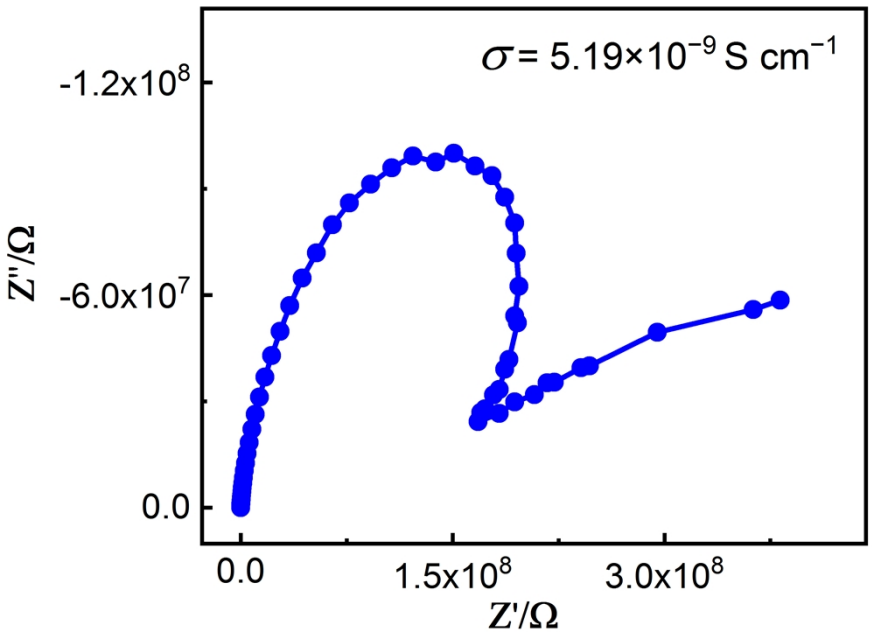

Figure S10. Nyquist plot for **1** at 85 °C under anhydrous condition

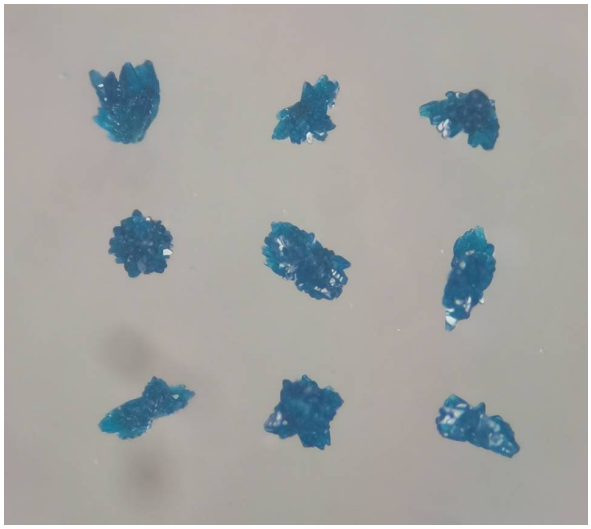

Figure S11. The photograph of crystals of **1** after proton conduction.

Figure S12. The photograph of crystals of **2** after proton conduction.

---

(1) Y. -B. Lu, J. Huang, X. -R. Yuan, S. -J. Liu, R. Li, H. -j. Liu, M. -P. Liu, H. -R. Wen, S. -D. Zhu and Y. -R. Xie, *Cryst. Growth. Des*., 2022, **22**, 1045–1053.